Contribution from the Department of Chemistry, University of Southern California, Los Angeles, California 90007

Molecular Structures of $H_4Ru_4(CO)_{12}$ and $H_4Ru_4(CO)_{10}(PPh_3)_2$

ROBERT D. WILSON, SU MIAU WU, RICHARD A. LOVE, and ROBERT BAU*

Received September 8, 1977

The structures of $H_4Ru_4(CO)_{12}$ and $H_4Ru_4(CO)_{10}(PPh_3)_2$ have been solved by single-crystal x-ray diffraction methods. Their geometries, like that of the closely related $H_4Ru_4(CO)_{11}P(OMe)_3$ reported earlier, consist of a distorted tetrahedral core (D_{2d} symmetry) with four long Ru–Ru distances and two short Ru–Ru distances. It is believed that the four H atoms, which were not unambiguously located in this study, bridge the four long edges of the Ru_4 cluster. In $H_4Ru_4(CO)_{12}$, $H_4Ru_4(CO)_{11}P(OMe)_3$, and $H_4Ru_4(CO)_{10}(PPh_3)_2$ the two short (nonbridged) Ru–Ru bonds are opposite each other, unlike those in $H_4Ru_4(CO)_{10}(Ph_2PCH_2CH_2PPh_2)$ which are ajacent to each other. All $H_4Ru_4(CO)_{12-n}L_n$ molecules investigated so far show carbonyl groups staggered with respect to the M–M edges of the M_4 cluster, in contrast to those in $H_4Re_4(CO)_{12}$ which are eclipsed. The structural analysis of $H_4Ru_4(CO)_{12}$ is complicated by packing disorder, which is commonly found in crystals of dodecacarbonyl metal cluster complexes. Structural details: in $H_4Ru_4(CO)_{12}$, the average long (Ru–H–Ru) and short (Ru–Ru) metal–metal distances are 2.950 (1) and 2.786 (1) Å, respectively; in $H_4Ru_4(CO)_{10}(PPh_3)_2$ they are 2.966 (2) and 2.772 (2) Å, respectively. Crystal details: $H_4Ru_4(CO)_{12}$ crystallizes in the triclinic space group $P\bar{1}$, with $a = 9.838$ (7) Å, $b = 10.087$ (6) Å, $c = 9.659$ (6) Å, $\alpha = 82.77$ (4)°, $\beta = 88.99$ (4)°, $\gamma = 85.08$ (3)°, $Z = 2$, and $V = 947.4$ Å^3; the final R factor was 6.3% for 4361 reflections ($I > 3\sigma$) collected at −175 °C. $H_4Ru_4(CO)_{10}(PPh_3)_2$ crystallizes in the monoclinic space group $P2_1/c$, with $a = 15.922$ (5) Å, $b = 17.888$ (7) Å, $c = 17.916$ (5) Å, $\beta = 112.04(2)$°, $Z = 4$, and $V = 4729.8$ Å^3; the final R factor was 6.5% for 3512 reflections ($I > 3\sigma$) collected at room temperature.

Introduction

In recent years work has dramatically proliferated in the area of metal hydrides,[1] particularly those with distinct molecular clusters such as polynuclear metal carbonyl hydrides[2] which may be more amenable to examination at atomic resolution than the (often nonstoichiometric) binary metal hydrides. At least four types of bonding modes have been established for hydrogen attached to multinuclear metal clusters. Besides terminally bonded (M–H) species, bridged compounds (M–H–M) are common, a number of triply bridging species (HM_3) exist, and even compounds having hydrogen atoms embedded in metal clusters have been found.[3] In bridging systems, it is informative to observe, apart from the metal–hydrogen coordination itself, the structural changes that the hydride bridges effect on the remainder of the molecule. We have recently shown how the arrangement of carbonyl groups in the "unsaturated" cluster $H_4Re_4(CO)_{12}$ can provide a clue as to the location of the hydride ligands in this molecule, together with other pieces of evidence such as the symmetry of the M_4 core itself.[4] In the present paper we extend our investigation to the "saturated" cluster $H_4Ru_4(CO)_{12}$ and its bis(triphenylphosphine) derivative.

The preparation of $H_4Ru_4(CO)_{12}$ was first reported in 1966 by Lewis,[5] Wilkinson,[6] and their co-workers and followed up by a joint publication shortly thereafter.[7] The various preparative routes included the treatment of $Ru_3(CO)_{12}$ with $NaBH_4$, sodium amalgam or KOH, and the high-pressure reductive carbonylation of a ruthenium chloride complex. A number of postulated structures for the compound were put forward by Johnson, Lewis, Wilkinson, and their colleagues:[7] structures having T_d, D_{2d}, and C_{3v} symmetry were specifically mentioned.[8] From the rather complex infrared spectrum of $H_4Ru_4(CO)_{12}$, however, it was immediately apparent to the authors that the symmetric T_d structure (with face-bridging hydrides) was highly improbable. Included in the original paper[7] is a description of the preparation of the related cluster complex $H_2Ru_4(CO)_{13}$, and soon thereafter the analogous osmium complexes $H_4Os_4(CO)_{12}$ and $H_2Os_4(CO)_{13}$ [together with $H_2Os_3(CO)_{12}$] were reported.[9,10]

In 1971 Kaesz and co-workers reported a novel synthetic approach to $H_4Ru_4(CO)_{12}$ which involved the direct hydrogenation of $Ru_3(CO)_{12}$ with gaseous H_2 at atmospheric pressure.[11] This new technique allows the preparation of $H_4Ru_4(CO)_{12}$ to reach near-quantitative levels and also enables $H_4Os_4(CO)_{12}$ and other metal cluster hydrides to be made with improved yields.[12] Subsequently, the preparation of phosphine and phosphite substituted derivatives improved solubility and allowed more extensive NMR investigations to be carried out.[13,14] For the series $H_4Ru_4(CO)_{12-n}L_n$ [L = $P(OCH_3)_3$, n = 1, 2, 3, 4], Knox and Kaesz found that the hydrogen ligands were equivalent on the NMR time scale and were also equivalently coupled to all the phosphorus nuclei in the molecule.[13] In that article the D_{2d} geometry for $H_4Ru_4(CO)_{12}$ and its derivatives (involving edge-bridging hydride ligands) was specifically proposed, and the phosphite ligands were assigned positions transoid to Ru–Ru bonds (i.e., the unbridged bonds). Kaesz and co-workers later reported the preparation of a deprotonated form of the complex, $[AsPh_4]^+[H_3Ru_4(CO)_{12}]^-$.[15]

Lately, there has been an increased activity in the properties of $H_4Ru_4(CO)_{12}$ as part of a general renewal of interest in metal clusters as catalysts.[16] Its presence was implicated in a new water gas shift reaction described by Laine, Rinker, and Ford,[17] and rearrangements in $H_4Ru_4(CO)_{12-n}L_n$ clusters are being actively pursued by Shapley and co-workers.[18]

$H_4Ru_4(CO)_{12}$, $H_4Os_4(CO)_{12}$, $H_2Ru_4(CO)_{13}$, and $H_2Os_4(CO)_{13}$ are all examples of electron-precise, or closed-shell, 60-electron clusters. In contrast, the reactive $H_4Re_4(CO)_{12}$ has four less electrons than $H_4Os_4(CO)_{12}$ and is considered electron deficient.[19] $H_4Re_4(CO)_{12}$ has a very simple two-band pattern in the infrared which is strongly suggestive of tetrahedral symmetry. $H_4Ru_4(CO)_{12}$ and $H_4Os_4(CO)_{12}$, on the other hand, have complex five-band patterns[12] and are clearly of lower symmetry. $H_2Ru_4(CO)_{13}$ and $H_2Os_4(CO)_{13}$ have even more complex spectra (seven bands).[7,9,20] In 1972 Yawney and Doedens reported the structure of $H_2Ru_4(CO)_{13}$ as that of a distorted tetrahedron, with four "short" Ru–Ru bonds of 2.78 (2) Å and two "long" Ru–Ru bonds of 2.93 (1) Å.[21] The two long bonds, which were adjacent to each other, were assigned hydrogen bridges.

Recently we showed that $H_4Re_4(CO)_{12}$ indeed has tetrahedral symmetry, with essentially equivalent Re–Re bond distances.[4] In that structure determination "Fourier-averaging" techniques were introduced to locate the hydrogen atoms on the faces of the tetrahedron. In the present paper we find that the Ru_4 cores of $H_4Ru_4(CO)_{12}$ and $H_4Ru_4(CO)_{10}(PPh_3)_2$ do not have tetrahedral symmetry, a fact which is consistent with edge-bridging positions for the hydride ligands. This conclusion was also reached earlier when we reported some preliminary results on $H_4Ru_4(CO)_{11}P(OMe)_3$.[22] A very recent report by Shapley and Churchill on the closely related $H_4Ru_4(CO)_{10}(Ph_2PCH_2CH_2PPh_2)$ also shows edge-

0020-1669/78/1317-1271$01.00/0

bridging hydrogen atoms,[18] but arranged in a different pattern from those in $H_4Ru_4(CO)_{12}$, $H_4Ru_4(CO)_{11}P(OMe)_3$, and $H_4Ru_4(CO)_{10}(PPh_3)_2$.

Experimental Section

Preparation of $H_4Ru_4(CO)_{12}$ and $H_4Ru_4(CO)_{10}(PPh_3)_2$. The parent dodecacarbonyl, $H_4Ru_4(CO)_{12}$, was prepared from $Ru_3(CO)_{12}$ using the direct hydrogenation procedure.[12] The phosphine derivative was then made by incomplete reaction with PPh_3 at 60 °C in hexane followed by column chromatographic separation from the other substituted products and unreacted parent carbonyl.[13] In a typical experiment $Ru_3(CO)_{12}$ (0.49 g, 0.76 mmol) was dissolved in approximately 100 ml of dry *n*-octane. Ultrapure grade H_2 gas (Matheson Co.) was bubbled through the solution under reflux for 2 h after which time only the five-band pattern[12] of $H_4Ru_4(CO)_{12}$ could be seen in the carbonyl stretching region of the infrared spectrum. This solution was cooled, evaporated to dryness under vacuum, redissolved in 100 mL of hexane (distilled from CaH_2/N_2), and filtered. The mixture was then treated dropwise with PPh_3 (0.20 g, 0.76 mmol) in 30 mL of hexane and heated to 60 °C for 2 h more. Although this corresponds to a 1:1 ratio of ligand to carbonyl compound, one does not simply get the monosubstituted product. Instead, substantial amounts of unreacted starting material are present together with mono-, di-, tri-, and sometimes even tetra-substituted products. The separation was accomplished on a silica gel column. Pure hexane eluted a yellow band of $H_4Ru_4(CO)_{12}$. Hexane/CH_2Cl_2 (16:1) eluted a second (small) pink band of $H_4Ru_4(CO)_{11}(PPh_3)$. The desired $H_4Ru_4(CO)_{10}(PPh_3)_2$ was eluted with hexane/CH_2Cl_2 (8:1) as a yellow-orange band. It was followed closely by a darker orange band of $H_4Ru_4(CO)_9(PPh_3)_3$. The $H_4Ru_4(CO)_{10}(PPh_3)_2$ band was collected and solvent removed in vacuo. The red residue was dissolved in CH_2Cl_2 which was then carefully removed at low pressure until the solution became just cloudy. The flask was then placed in a freezer overnight to produce the crystals used in the x-ray analysis.

The yellow-orange $H_4Ru_4(CO)_{12}$ is somewhat air and moisture stable, moderately soluble in hydrocarbons, but more soluble in CH_2Cl_2. Although recrystallized most often as a microcrystalline powder, diligent effort can yield good quality, albeit small, single crystals suitable for x-ray analysis out of slowly cooled CH_2Cl_2 solutions. The compound was identified by its IR spectrum (hexane solution) in the carbonyl stretching region [2075 cm^{-1} (s), 2062 cm^{-1} (vs), 2025 cm^{-1} (m), 2019 cm^{-1} (s), 2005 cm^{-1} (w)], in good agreement with the literature values.[12] Care must be taken to avoid mistaking $Ru_3(CO)_{12}$ for $H_4Ru_4(CO)_{12}$ since they chromatograph very similarly and incomplete reaction in the initial step will ensure their simultaneous presence in solution. The experienced hand can manually separate the larger, more regular orange crystals of $Ru_3(CO)_{12}$ from the yellow-orange aggregates of $H_4Ru_4(CO)_{12}$ in cases of cocrystallization.

Data Collection and Structure Analysis of $H_4Ru_4(CO)_{10}(PPh_3)_2$. A dark red crystal of $H_4Ru_4(CO)_{10}(PPh_3)_2$ (approximate dimensions 0.34 × 0.42 × 0.60 mm) was mounted in air on a glass fiber. Precession photographs indicated a monoclinic crystal system with systematic absences consistent with space group $P2_1/c$ (No. 14). The unit cell parameters, which are given in Table I together with other crystallographic details, were obtained by carefully measuring the setting angles of 29 reflections on a Nonius CAD-3 automated diffractometer. One quadrant of data (with some duplicate reflections) were collected by a θ–2θ scan technique using Zr-filtered Mo Kα radiation up to a 2θ limit of 45°. The details of data collection are essentially the same as those given in an earlier publication.[23] The scan was set at $\Delta\theta = (1.2 + 0.15 \tan\theta)°$. As a check of the stability of the diffractometer and the crystal, the (0,12,0), (11,0,0) and ($\bar{4}$,0,12) reflections were measured at 50-reflection intervals and were found to be stable. The 4600 reflections were corrected for Lorentz and polarization effects and merged. An empirical absorption correction was applied to the data based on the variation in intensity of an axial reflection (at $\chi = 90°$) with the spindle angle ϕ.[24a] The transmission factors obtained in this manner ranged from 0.944 to 1.044 (normalized to unity). The 3512 reflections remaining after data reduction (with $I > 3\sigma$) were used for the subsequent structure analysis. The standard deviation of each intensity reading, $\sigma(I)$, was estimated using the expression $\sigma(I) = [(\text{peak} + \text{background counts}) + 0.04^2(\text{net intensity})^2]^{1/2}$.[24b]

From an analysis of the peaks of a three-dimensional Patterson map, the positions of the four ruthenium atoms (0.11, 0.22, 0.20), (0.30, 0.22, 0.27), (0.19, 0.37, 0.22), and (0.19, 0.29, 0.35) were determined. A difference Fourier map phased by these atoms revealed the positions of the two phosphorus atoms and fragments of the carbonyl and phenyl groups. Four successive difference Fourier maps based on structure factor calculations phased by an increasing number of atoms led to the unambiguous locations of all nonhydrogen atoms. After the rigid-body parameters of the six benzene rings were calculated,[25] they were varied in two cycles of isotropic least-squares refinement together with all the other nonhydrogen atoms in the molecule.[26a] This was followed by six more refinement cycles in which the Ru and P atoms were assigned anisotropic thermal parameters. At this stage, the refinement was discontinued since each of the calculated shifts was less than one-tenth of the corresponding standard deviation. The final agreement factors were $R = 6.5\%$ and $R_w = 9.3\%$.[26b] A final difference Fourier showed no unexpected features. No indication of the hydride ligands was obtained from this map.

Table I. Crystal Data for $H_4Ru_4(CO)_{12}$ and $H_4Ru_4(CO)_{10}(PPh_3)_2$

	$H_4Ru_4(CO)_{12}$	$H_4Ru_4(CO)_{10}(PPh_3)_2$
Crystal type	Triclinic	Monoclinic
Space group	$P\bar{1}$	$P2_1/c$
Cell constants[a]		
a, A	9.838 (7)	15.922 (5)
b, A	10.087 (6)	17.888 (7)
c, A	9.659 (6)	17.916 (5)
α, deg	82.77 (4)	90.0
β, deg	88.99 (4)	112.04 (2)
γ, deg	85.08 (3)	90.0
V,[a] A^3	947.4	4729.8
Z	2	4
Temp of data collection, °C	−175	~25
Mol wt	744.4	1213.0
Calcd density,[b] g cm^{-3}	2.51	1.70
Obsd density,[b] g cm^{-3}	2.50	1.69
μ(Mo Kα), cm^{-1}	31.10	13.41
Size of crystal, mm	0.15 × 0.25 × 0.31	0.34 × 0.42 × 0.60
Variation in transmission coeff[c]	0.972–1.036	0.944–1.044
Data collected	One hemisphere	One quadrant
2θ upper limit used, deg	60	45
No. of reflections used	4361	3512
Final R factor, %	6.3	6.5

[a] Unit cell parameters and cell volume for $H_4Ru_4(CO)_{12}$ given in the table correspond to −175 °C, the temperature used in data collection. At room temperature, the following unit cell parameters were obtained: $a = 9.98$ (5) A, $b = 10.16$ (4) A, $c = 9.82$ (5) A, $\alpha = 82.6$ (3)°, $\beta = 88.9$ (2)°, $\gamma = 85.9$ (2)°, $V = 985$ A^3. [b] The calculated and observed densities are given at room temperature. At −175 °C, the calculated density for $H_4Ru_4(CO)_{12}$ is 2.609 g cm^{-3}. [c] Transmission coefficients are normalized to an average of unity.

Data Collection and Structure Analysis of $H_4Ru_4(CO)_{12}$. The specimen studied was a small piece cleaved from a polycrystalline aggregate. The single crystal obtained, a trapezoidal plate having a depth of ~0.15 mm and parallel side dimensions of ~0.10 and ~0.25 mm with a ~0.31 mm perpendicular separation, was mounted on the tip of a tapered glass fiber. Since $H_4Ru_4(CO)_{11}(P(OMe)_3)$[22] and $H_4Ru_4(CO)_{10}(PPh_3)_2$ had already undergone crystallographic analysis, it was decided that the parent dodecacarbonyl should be studied at low temperature in an attempt to get molecular parameters of a higher precision. Additionally, our recent success at applying "Fourier-averaging" techniques to $H_4Re_4(CO)_{12}$[4] made us anxious to try these on another highly symmetric cluster hydride complex. Extensive low-temperature data were therefore collected. Preliminary room-temperature precession photos indicated a triclinic space group, but threefold Laue symmetry was approximated (see caption to Figure 3). Six Friedel-related pairs of reflections centered at room temperature and twelve pairs at −175 °C result in the unit cell parameters of Table I after least-squares refinement.

Acquisition and processing of diffraction data were as described earlier with the following additional details: (i) A Nonius Universal Low Temperature Device which blows a cold dry stream of N_2 gas over the sample was employed. The diffractometer was housed in

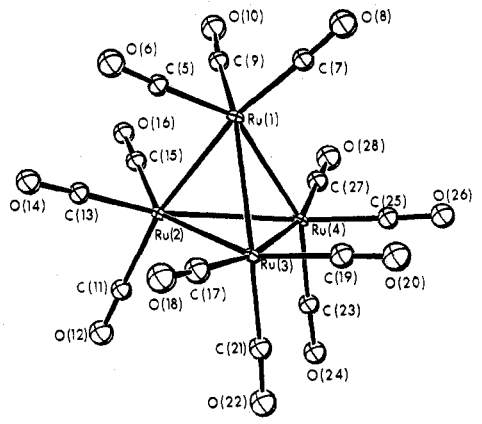

Figure 1. Molecular plot of $H_4Ru_4(CO)_{12}$ depicting the location of carbonyls trans to Ru–Ru edges. Hydrogen atoms (not shown) bridge edges Ru(1)–Ru(3), Ru(1)–Ru(4), Ru(2)–Ru(3), and Ru(2)–Ru(4) of the distorted tetrahedron. Thermal ellipsoids correspond to 50% probability.

a tent which was slowly and constantly flushed with dry room-temperature N_2 to minimize ice formation around the sample. (ii) Temperature stability was acceptable at -175 ± 3 °C for the 12-day experimental period as found by frequent monitoring of the cold stream ~0.8 cm upstream of the crystal with a Ni–Al/Ni–Cr (calibrated) thermocouple. (iii) High-range θ–2θ scans measured during periods of some visible crystal frosting failed to show observable ice powder pattern peaks. (iv) One hemisphere of data was collected to a 2θ limit of 60° using Zr-filtered Mo Kα x rays. (v) The scan cycle was repeated a maximum of six times for any reflection. (vi) The scan range was increased to $[1.5 + 0.15 \tan \theta_{hkl}]°$. (vii) One of the check reflections (005), (0$\bar{5}$0), ($\bar{5}$00) was recorded once every 60 measurements. Two of these standards were quite stable but the (005) reflection (at $\chi \approx 0°$) steadily decreased in intensity by 21% while remaining well centered. No "anisotropic decay" scaling was applied to fit this puzzling anomaly. In all, 6031 reflection intensities were recorded, affording 4361 unique observables ($I > 3\sigma(I)$) after processing which included empirical absorption corrections[24a] (transmission coefficient range 1.036–0.972).

Using heavy-atom methods this structure was successfully solved in space group $P\bar{1}$. After two cycles of least-squares refinement on the scale factor and the coordinates of the four metals located in the Patterson map, a difference Fourier synthesis clearly revealed all carbonyl positions. Refinement, with all thermal parameters varied isotropically, reduced the residual index (R) to 8.7%. Two further refinement cycles with the metal treated as anisotropically vibrating atoms lowered R to 7.9% and a ΔF map generated at this stage disclosed four compact regions of pronounced electron density (average 6.7 e Å^{-3}). The first interpretation was that these were hydride ligands with very little thermal motion, but after calculating the bond distances it was clear that this represented another orientation of the tetramer occurring in a small fraction of the sites. This calculation revealed the characteristic four-long/two-short pattern of M–M distances we had come to expect for H_4Ru_4 clusters. Several subsequent cycles of population refinement[27] resulted in successful convergence of all atomic parameters and yielded a model having a molecule in one orientation in 96.7 (2)% of the unit cells and in a second orientation in the rest of the unit cells.

Verification of the expected edge-bridging hydride locations by location in ΔF maps was next tried. Image-enhancing techniques as were used with $H_4Re_4(CO)_{12}$[4] were attempted here with anticipated success since (i) Ru is only a second-row transition metal and (ii) with −175 °C data, the reduced thermal motion should yield smaller and hence denser H atom peaks. Indeed a peak (0.52 e Å^{-3} compared to 1.4 e Å^{-3} for metal residuals, using all data) was found in the expected site with a measured Ru–H distance of 1.76 Å (Figure 6). This, however, was inconclusive since the "H" peak decreases in relation to metal residuals as more and more high-angle data are omitted in the calculations, just contrary to expectation.[28] Additionally, it is difficult to attach much significance to this observation due to the partial molecular disordering which leads to the 3% Ru atoms conceivably masking the alternative triply bridging sites for the hydride ligands. The final discrepancy indices in this heavily overdetermined

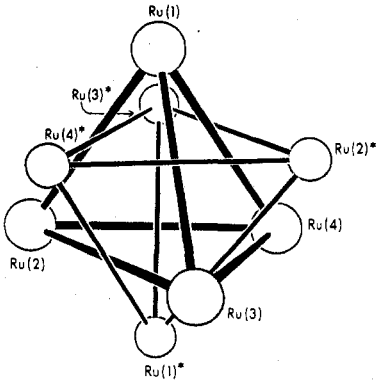

Figure 2. Configuration of the metal tetramer core in $H_4Ru_4(CO)_{12}$ portraying the 97%–3% disordering of the molecules.

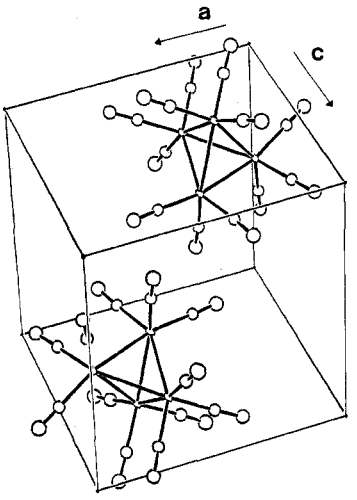

Figure 3. Unit cell plot for $H_4Ru_4(CO)_{12}$ (omitting the 3% disordered molecule). Note the approximate crystallographic threefold axis (body diagonal), passing through both molecules. This is substantiated by the Ru coordinates (Table II) that are approximately of the form w, w, w; x, y, z; y, z, x; z, x, y. This outcome was anticipated from the preliminary precession pictures in which three zero-layer photos taken at ~120° intervals of the spindle angle showed very similar diffraction patterns.

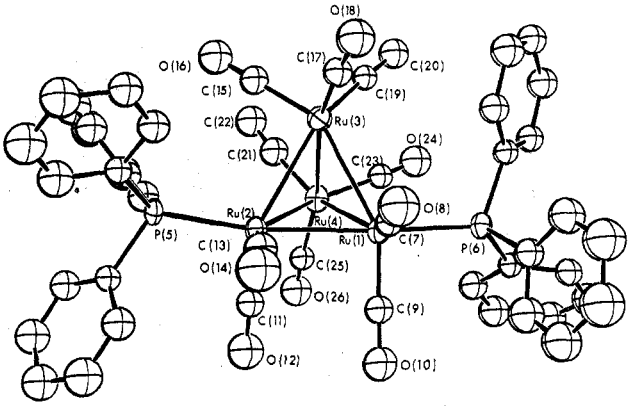

Figure 4. Molecular plot of $H_4Ru_4(CO)_{10}(PPh_3)_2$. Again, hydrogen atoms (not shown) bridge edges Ru(1)–Ru(3), Ru(1)–Ru(4), Ru(2)–Ru(3), and Ru(2)–Ru(4). The staggered configuration of the carbonyl groups with respect to the Ru–Ru edges is clearly evident around atom Ru(4).

analysis (the data-to-parameter ratio is over 29) are R = 6.3% and R_w = 7.4%.[26b]

Results and Discussion

The final atomic positions, distances and angles for $H_4Ru_4(CO)_{12}$ and $H_4Ru_4(CO)_{10}(PPh_3)_2$ are listed in Tables II–VII. Various molecular plots are shown in Figures 1–6,

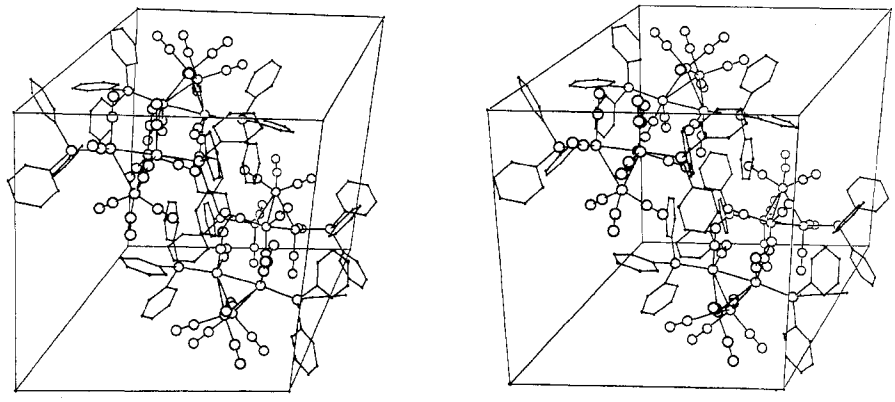

Figure 5. A stereoscopic plot of the unit cell of $H_4Ru_4(CO)_{10}(PPh_3)_2$. The *a* axis is horizontal, the *b* axis is vertical, and the *c* axis comes out of the plane of the paper.

Table II. Final Atomic Parameters for $H_4Ru_4(CO)_{12}$

(A) Positional Parameters and Isotropic Temperature Factors[b]

Atom	*x*	*y*	*z*	*B*, Å^2
Ru(1)[a]	0.33838 (6)	0.34521 (6)	0.34899 (6)	
Ru(2)[a]	0.07714 (5)	0.32535 (6)	0.25165 (6)	
Ru(3)[a]	0.25886 (6)	0.07713 (6)	0.30945 (6)	
Ru(4)[a]	0.31282 (5)	0.25435 (6)	0.07331 (6)	
C(5)	0.2662 (8)	0.3650 (8)	0.5297 (8)	1.32 (11)
O(6)	0.2269 (6)	0.3770 (6)	0.6390 (6)	2.02 (10)
C(7)	0.5303 (8)	0.3280 (8)	0.4003 (8)	1.24 (11)
O(8)	0.6389 (7)	0.3197 (6)	0.4320 (6)	2.10 (10)
C(9)	0.3304 (8)	0.5324 (8)	0.2886 (8)	1.36 (11)
O(10)	0.3318 (7)	0.6443 (6)	0.2494 (6)	2.07 (10)
C(11)	−0.0871 (8)	0.2786 (8)	0.1666 (8)	1.43 (11)
O(12)	−0.1823 (6)	0.2520 (6)	0.1185 (7)	2.04 (10)
C(13)	−0.0072 (8)	0.3357 (8)	0.4294 (8)	1.27 (11)
O(14)	−0.0611 (6)	0.3411 (6)	0.5327 (6)	1.81 (10)
C(15)	0.0466 (8)	0.5126 (8)	0.1949 (8)	1.39 (11)
O(16)	0.0254 (6)	0.6238 (6)	0.1571 (6)	1.59 (9)
C(17)	0.2041 (9)	−0.0115 (8)	0.4872 (8)	1.70 (12)
O(18)	0.1689 (7)	−0.0589 (7)	0.5930 (7)	2.23 (11)
C(19)	0.4314 (8)	−0.0240 (8)	0.3003 (8)	1.55 (12)
O(20)	0.5310 (7)	−0.0867 (7)	0.2974 (7)	2.24 (11)
C(21)	0.1757 (8)	−0.0331 (8)	0.1963 (8)	1.60 (12)
O(22)	0.1216 (7)	−0.0999 (7)	0.1320 (7)	2.19 (10)
C(23)	0.2275 (8)	0.1589 (8)	−0.0560 (8)	1.33 (11)
O(24)	0.1801 (6)	0.1041 (6)	−0.1362 (6)	1.70 (9)
C(25)	0.4854 (8)	0.1641 (8)	0.0459 (8)	1.35 (11)
O(26)	0.5908 (6)	0.1129 (6)	0.0266 (6)	1.81 (9)
C(27)	0.3430 (8)	0.4087 (8)	−0.0602 (8)	1.47 (11)
O(28)	0.3671 (7)	0.4989 (7)	−0.1338 (7)	2.31 (11)
Ru(1*)[a]	0.1490 (15)	0.1599 (15)	0.1653 (15)	0.33 (25)
Ru(2*)[a]	0.4292 (13)	0.1804 (13)	0.2500 (13)	−0.04 (23)
Ru(3*)[a]	0.2632 (15)	0.4200 (15)	0.1786 (15)	0.28 (25)
Ru(4*)[a]	0.1935 (14)	0.2383 (14)	0.4259 (14)	0.15 (25)

(B) Anisotropic Temperature Factors[b,c]

Atom	$10^5\beta_{11}$	$10^5\beta_{22}$	$10^5\beta_{33}$	$10^5\beta_{12}$	$10^5\beta_{13}$	$10^5\beta_{23}$
Ru(1)	171 (5)	187 (5)	255 (5)	−91 (4)	−6 (4)	−64 (4)
Ru(2)	135 (5)	186 (5)	266 (5)	−65 (4)	11 (4)	−64 (4)
Ru(3)	172 (5)	156 (5)	316 (6)	−75 (4)	24 (4)	−44 (4)
Ru(4)	146 (5)	196 (5)	251 (5)	−82 (4)	23 (4)	−74 (4)

[a] There is a slight amount of packing disorder in the molecule. Atoms Ru(1), Ru(2), Ru(3), and Ru(4) have an occupancy factor of 96.7 (2)%, while atoms Ru(1*), Ru(2*), Ru(3*), and Ru(4*) have an occupancy factor of 3.3 (2)%. All other atoms were assigned a 100% population factor. [b] The low values for the *B*'s and β's in this table reflect the low temperature used in data collection (−175 ± 3 °C). [c] The form of the anisotropic Debye-Waller factor is $\exp[-(\beta_{11}h^2 + \beta_{22}k^2 + \beta_{33}l^2 + 2\beta_{12}hk + 2\beta_{13}hl + 2\beta_{23}kl)]$.

and listings of observed and calculated structure factors are available.[30]

The dominant structural feature in both molecules is the characteristic four-long/two-short pattern of Ru–Ru distances

Table III. Bond Distances (Å) in $H_4Ru_4(CO)_{12}$

(a) Ru–Ru (Long) Distances

Ru(1)–Ru(3)	2.9502 (9)	Ru(2)–Ru(3)	2.9483 (8)
Ru(1)–Ru(4)	2.9446 (8)	Ru(2)–Ru(4)	2.9565 (7)
		Av	2.9499 (8)[a]

(b) Ru–Ru (Short) Distances

Ru(1)–Ru(2)	2.7839 (8)	Ru(3)–Ru(4)	2.7881 (8)
		Av	2.7860 (8)[a]

(c) Ru–Ru (Long) Distances in the 3% Occupancy Molecule

Ru(1*)–Ru(3*)	2.913 (19)	Ru(2*)–Ru(3*)	2.922 (20)
Ru(1*)–Ru(4*)	2.931 (20)	Ru(2*)–Ru(4*)	2.959 (21)
		Av	2.93 (2)[a]

(d) Ru–Ru (Short) Distances in the 3% Occupancy Molecule

Ru(1*)–Ru(2*)	2.784 (20)	Ru(3*)–Ru(4*)	2.815 (20)
		Av	2.80 (2)[a]

(e) Ru–C (Pseudo-Trans to the Long M–M Bonds) Distances

Ru(1)–C(5)	1.901 (8)	Ru(3)–C(19)	1.910 (8)
Ru(1)–C(9)	1.900 (8)	Ru(3)–C(21)	1.896 (8)
Ru(2)–C(13)	1.904 (7)	Ru(4)–C(23)	1.915 (8)
Ru(2)–C(15)	1.899 (8)	Ru(4)–C(25)	1.887 (8)
		Av	1.902 (3)[a]

(f) Ru–C (Pseudo-Trans to the Short M–M Bonds) Distances

Ru(1)–C(7)	1.948 (8)	Ru(3)–C(17)	1.924 (8)
Ru(2)–C(11)	1.945 (8)	Ru(4)–C(27)	1.933 (8)
		Av	1.938 (8)[a]

(g) Carbonyl Distances

C(5)–O(6)	1.134 (10)	C(17)–O(18)	1.134 (11)
C(7)–O(8)	1.110 (10)	C(19)–O(20)	1.122 (11)
C(9)–O(10)	1.145 (10)	C(21)–O(22)	1.140 (11)
C(11)–O(12)	1.120 (10)	C(23)–O(24)	1.135 (10)
C(13)–O(14)	1.127 (10)	C(25)–O(26)	1.141 (10)
C(15)–O(16)	1.138 (10)	C(27)–O(28)	1.121 (11)
		Av	1.131 (3)[a]

[a] See footnote 29.

that had been previously found in $H_4Ru_4(CO)_{11}P(OMe)_3$.[22] In all three molecules, the two short distances are located opposite each other. If one makes the usual assumption[31,32] that the long distances correspond to Ru–H–Ru bonds and the short distances to unbridged Ru–Ru bonds, one obtains the D_{2d} structure (I) originally proposed by Knox and Kaesz.[13] This is consistent with (i) the Raman spectrum which indicates nonlinear bridged M–H–M features,[12] and (ii) the five-band ν_{CO} infrared spectrum expected for D_{2d} symmetry. Interestingly, in a recent structure determination of the closely related compound $H_4Ru_4(CO)_{10}(Ph_2PCH_2CH_2PPh_2)$ by Churchill, Shapley, and co-workers,[18] the two short Ru–Ru bonds were found to be *adjacent* to each other (II). In $H_4Ru_4(CO)_{10}(Ph_2PCH_2CH_2PPh_2)$ the hydrogen atoms *were* successfully located crystallographically.

The existence of these two structural forms (I and II) lends support to the conclusions derived from NMR data[13,18] which

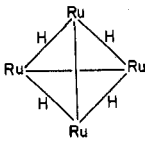

I

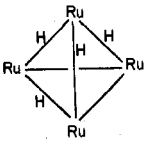

II

indicate that the H atoms of the H_4Ru_4 core can readily tautomerize between the various edge-bridging positions of the Ru_4 tetrahedron. Structural details of the various $H_4Ru_4(CO)_{12-n}L_n$ molecules are summarized in Table VIII.

The long (Ru–H–Ru) and short (Ru–Ru) metal–metal distances in $H_4Ru_4(CO)_{12-n}L_n$-type molecules agree quite well with each other (Table VIII). The long distances (average 2.944 Å) compare favorably with those in $H_2Ru_4(CO)_{13}$ (2.930 Å),[21] and even with the triply bridged (μ_3-H) Ru–Ru separation in $H_2Ru_6(CO)_{18}$ (2.954 Å).[32] The short (nonbridged) Ru–Ru distances (average 2.780 Å), however, are significantly different from those of many other Ru–Ru single bonds. Although they agree well with those of $H_2Ru_4(CO)_{13}$ (2.784 Å),[21] they are distinctly shorter than the nonbridged Ru–Ru distances in $H_2Ru_6(CO)_{18}$ (2.867 Å),[32] $Ru_3(CO)_6(\eta^5\text{-}C_8H_9)(\eta^7\text{-}C_8H_9)$ (2.84 Å),[33] and $Ru_3(CO)_{12}$ itself (2.854 Å).[34]

The entire molecular geometry of $H_4Ru_4(CO)_{12}$ closely conforms to D_{2d} symmetry. One can see two noncrystallographic mirror planes in the molecule and not six (as would be expected for T_d symmetry). Two kinds of metal–carbon bonds are found. Those opposite an unbridged Ru–Ru bond are consistently longer [Ru–C = 1.938 (8) Å average] than those opposite a bridged Ru–H–Ru bond [Ru–C = 1.902 (3) Å average]. Additionally, the Ru–C bonds opposite an unbridged Ru–Ru edge are more collinear with that edge [Ru–Ru–C = 167.7 (2)° average] than those opposite a hydrogen-bridged Ru–Ru edge [Ru–Ru–C = 151.1 (6)° average]. No significant difference was seen in the carbonyls themselves [C–O = 1.131 (3) Å average], and they are all coordinated essentially linearly [Ru–C–O = 177.6 (2)° average]. Note the systematic alternation in the temperature factors of the carbonyl groups (Table II): the isotropic thermal parameters of the carbon atoms are all consistently lower than those of the oxygen atoms.

Trends in M–C bond lengths ("the structural trans effect") have been studied by Ibers and Coyle.[35] They have noted that M–L distances opposite π-bonding ligands (such as CO) are longer than M–L distances opposite σ-bonding ligands (such as H). This effect has been attributed to a greater competition for back-bonding electrons (and a concomitant weakening of the M–L bonds) when two π-bonding ligands are opposite each other. In the case of $H_4Ru_4(CO)_{12}$, the fact that Ru–C bonds opposite nonbridged Ru–Ru bonds are longer than those opposite Ru–H–Ru bonds would imply that the Ru–Ru bond is a better "π ligand" than the Ru–H–Ru bridge bond.

It was largely the 97%–3% packing disorder in $H_4Ru_4(CO)_{12}$ (see Figure 2) which prevented us from successfully applying "image-enhancing" techniques that we had earlier used to locate the hydrogen atoms in $H_4Re_4(CO)_{12}$.[4] Dodecacarbonyl metal clusters are notoriously prone to pack in a disordered fashion, as has been pointed out by Wei and Dahl in their classic investigations of $Fe_3(CO)_{12}$, $Co_4(CO)_{12}$, and $Rh_4(CO)_{12}$.[36] We had also experienced this phenomenon in our investigation of the structure of the $[H_6Re_4(CO)_{12}]^{2-}$ anion.[37]

The gross geometry of the ruthenium–carbonyl skeleton of $H_4Ru_4(CO)_{10}(PPh_3)_2$ is very similar to that of $H_4Ru_4(CO)_{12}$. The presence of the phosphine groups has made only subtle changes in the geometry of the rest of the molecule: for example, the Ru–Ru–C angles show a larger variation in $H_4Ru_4(CO)_{10}(PPh_3)_2$ (Table VIIh) than in $H_4Ru_4(CO)_{12}$ (Table IVh), presumably because of the perturbing influence of the bulky phosphine groups.

The configurations of $H_4Ru_4(CO)_{12}$, $H_4Ru_4(CO)_{11}P(OMe)_3$, and $H_4Ru_4(CO)_{10}(PPh_3)_2$ can be concisely represented in III. It can be seen that the phosphine or phosphite

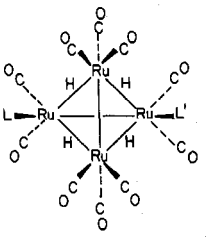

III

$H_4Ru_4(CO)_{12}$: L = L' = CO
$H_4Ru_4(CO)_{11}P(OMe)_3$: L = CO, L' = $P(OMe)_3$
$H_4Ru_4(CO)_{10}(PPh_3)_2$: L = L' = PPh_3

ligands are found in positions transoid to a short (unbridged) Ru–Ru bond, as expected from IR and NMR data.[13] For $H_4Ru_4(CO)_{10}(Ph_2PCH_2CH_2PPh_2)$, however, the two P atoms of the diphos ligand are sterically prevented by the ethylene bridge to be mutually transoid to any given Ru–Ru edge. The bidentate ligand was found to chelate the unique ruthenium atom which is involved in three Ru–H–Ru bridge bonds.[18] This necessarily means that, unlike the other $H_4Ru_4(CO)_{12-n}L_n$ complexes, the phosphorus atoms of $H_4Ru_4(CO)_{10}$(diphos) are transoid to Ru–H–Ru bonds (IV). Just about the only thing

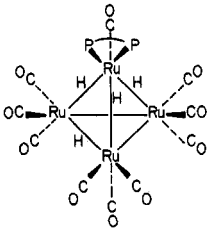

IV

common between structures III and IV is that each phosphorus atom is cisoid to two Ru–H–Ru bonds.

The carbonyl groups in all $H_4Ru_4(CO)_{12-n}L_n$ molecules investigated so far are staggered with respect to the metal–metal edges (V), in contrast to those in $H_4Re_4(CO)_{12}$ which are eclipsed (VI). The staggered conformation is best seen

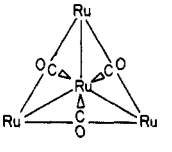

V

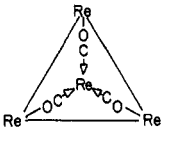

VI

in Figure 4 [note in particular the coordination about atom Ru(4)]. In the case of $H_4Re_4(CO)_{12}$, we pointed out[4] that the configuration of the CO groups can serve as a useful indicator for the location of the hydrogen atoms in the cluster. This idea is based on the simple premise that the basic "building block" in these molecules is the octahedral $M(CO)_3$ unit with three "available" orbitals (VII). Hoffmann and co-workers

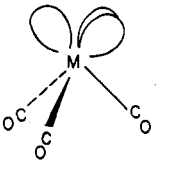

VII

have found this simple concept useful in describing the bonding

Table IV. Bond Angles (deg) in $H_4Ru_4(CO)_{12}$

	(a) Ru-(short)-Ru-(long)-Ru Angles		
Ru(2)-Ru(1)-Ru(3)	61.80 (2)	Ru(1)-Ru(3)-Ru(4)	61.67 (2)
Ru(2)-Ru(1)-Ru(4)	62.07 (2)	Ru(2)-Ru(3)-Ru(4)	61.97 (2)
Ru(1)-Ru(2)-Ru(3)	61.87 (2)	Ru(1)-Ru(4)-Ru(3)	61.87 (2)
Ru(1)-Ru(2)-Ru(4)	61.64 (2)	Ru(2)-Ru(4)-Ru(3)	61.68 (2)
		Av	61.82 (5)[a]
	(b) Ru-(long)-Ru-(long)-Ru Angles		
Ru(3)-Ru(1)-Ru(4)	56.45 (2)	Ru(1)-Ru(3)-Ru(2)	56.33 (2)
Ru(3)-Ru(2)-Ru(4)	56.35 (2)	Ru(1)-Ru(4)-Ru(2)	56.30 (2)
		Av	56.36 (2)[a]
	(c) Ru-(short)-Ru-(long)-Ru Angles in the 3% Occupancy Molecule		
Ru(2*)-Ru(1*)-Ru(3*)	61.7 (5)	Ru(1*)-Ru(2*)-Ru(3*)	61.3 (5)
Ru(2*)-Ru(1*)-Ru(4*)	62.3 (5)	Ru(1*)-Ru(2*)-Ru(4*)	61.3 (5)
Ru(1*)-Ru(3*)-Ru(4*)	61.5 (5)	Ru(1*)-Ru(4*)-Ru(3*)	60.9 (5)
Ru(2*)-Ru(3*)-Ru(4*)	62.1 (5)	Ru(2*)-Ru(4*)-Ru(3*)	60.7 (5)
		Av	61.5 (2)[a]
	(d) Ru-(long)-Ru-(long)-Ru Angles in the 3% Occupancy Molecule		
Ru(3*)-Ru(1*)-Ru(4*)	57.6 (5)	Ru(3*)-Ru(2*)-Ru(4*)	57.2 (5)
Ru(1*)-Ru(3*)-Ru(2*)	57.0 (5)	Ru(1*)-Ru(4*)-Ru(2*)	56.4 (5)
		Av	57.1 (5)[a]
	(e) Ru-(short)-Ru-C (Pseudo-Trans) Angles		
Ru(2)-Ru(1)-C(7)	168.9 (2)	Ru(1)-Ru(2)-C(11)	167.8 (2)
Ru(4)-Ru(3)-C(17)	167.8 (3)	Ru(3)-Ru(4)-C(27)	166.4 (2)
		Av	167.7 (2)[a]
	(f) Ru-(short)-Ru-C (Pseudo-Cis) Angles		
Ru(2)-Ru(1)-C(5)	90.2 (2)	Ru(1)-Ru(2)-C(13)	94.0 (2)
Ru(2)-Ru(1)-C(9)	92.4 (2)	Ru(1)-Ru(2)-C(15)	93.4 (2)
Ru(4)-Ru(3)-C(19)	93.3 (2)	Ru(3)-Ru(4)-C(23)	95.7 (2)
Ru(4)-Ru(3)-C(21)	90.1 (2)	Ru(3)-Ru(4)-C(25)	92.5 (2)
		Av	92.7 (7)[a]
	(g) Ru-(long)-Ru-C (Pseudo-Trans) Angles		
Ru(3)-Ru(1)-C(9)	149.2 (2)	Ru(3)-Ru(2)-C(15)	151.8 (2)
Ru(4)-Ru(1)-C(5)	150.0 (2)	Ru(4)-Ru(2)-C(13)	151.9 (2)
Ru(1)-Ru(3)-C(21)	148.6 (3)	Ru(1)-Ru(4)-C(23)	152.8 (2)
Ru(2)-Ru(3)-C(19)	152.7 (3)	Ru(2)-Ru(4)-C(25)	151.8 (2)
		Av	151.1 (6)[a]
	(h) Ru-(long)-Ru-C (Pseudo-Cis) Angles		
Ru(3)-Ru(1)-C(7)	108.3 (2)	Ru(3)-Ru(2)-C(11)	107.3 (2)
Ru(4)-Ru(1)-C(7)	109.0 (2)	Ru(4)-Ru(2)-C(11)	108.2 (2)
Ru(1)-Ru(3)-C(17)	108.5 (3)	Ru(1)-Ru(4)-C(27)	105.2 (2)
Ru(2)-Ru(3)-C(17)	107.0 (3)	Ru(2)-Ru(4)-C(27)	108.4 (2)
		Av	107.7 (4)[a]
	(i) Ru-(long)-Ru-C (Pseudo-Cis) Angles		
Ru(3)-Ru(1)-C(5)	101.6 (2)	Ru(3)-Ru(2)-C(13)	101.1 (2)
Ru(4)-Ru(1)-C(9)	97.7 (2)	Ru(4)-Ru(2)-C(15)	101.1 (2)
Ru(1)-Ru(3)-C(19)	102.4 (3)	Ru(1)-Ru(4)-C(25)	103.1 (2)
Ru(2)-Ru(3)-C(21)	99.7 (3)	Ru(2)-Ru(4)-C(23)	100.7 (2)
		Av	100.9 (6)[a]
	(j) C-Ru-C Angles		
C(5)-Ru(1)-C(7)	96.9 (3)	C(17)-Ru(3)-C(19)	96.2 (3)
C(5)-Ru(1)-C(9)	94.7 (3)	C(17)-Ru(3)-C(21)	97.3 (4)
C(7)-Ru(1)-C(9)	95.4 (3)	C(19)-Ru(3)-C(21)	92.0 (4)
C(11)-Ru(2)-C(13)	93.9 (3)	C(23)-Ru(4)-C(25)	92.4 (3)
C(11)-Ru(2)-C(15)	95.4 (3)	C(23)-Ru(4)-C(27)	95.4 (3)
C(13)-Ru(2)-C(15)	93.7 (3)	C(25)-Ru(4)-C(27)	94.9 (3)
		Av	94.9 (5)[a]
	(k) Ru-C-O Angles		
Ru(1)-C(5)-O(6)	178.0 (7)	Ru(3)-C(17)-O(18)	177.2 (8)
Ru(1)-C(7)-O(8)	178.4 (7)	Ru(3)-C(19)-O(20)	177.8 (7)
Ru(1)-C(9)-O(10)	176.6 (7)	Ru(3)-C(21)-O(22)	177.3 (7)
Ru(2)-C(11)-O(12)	179.4 (7)	Ru(4)-C(23)-O(24)	177.6 (7)
Ru(2)-C(13)-O(14)	177.7 (7)	Ru(4)-C(25)-O(26)	177.9 (7)
Ru(2)-C(15)-O(16)	177.5 (7)	Ru(4)-C(27)-O(28)	176.1 (7)
		Av	177.6 (2)[a]

[a] See footnote 29.

in many metal carbonyl complexes.[38]

Thus, in the staggered conformation V the three metal orbitals are directed at the edges of the tetrahedron, while in the eclipsed conformation VI they are directed at the faces. This provides a plausible rationalization for the edge-bridging positions of the H atoms in $H_4Ru_4(CO)_{12}$ as opposed to the face-bridging hydrogens in $H_4Re_4(CO)_{12}$. An interesting case for comparison is $H_2Ru_6(CO)_{18}$.[32] Although the primary

Table V. Final Atomic Parameters for $H_4Ru_4(CO)_{10}(PPh_3)_2$

(A) Positional Parameters and Isotropic Temperature Factors

Atom	*x*	*y*	*z*	*B*, Å^2
Ru(1)	0.10518 (7)	0.21615 (6)	0.19353 (6)	
Ru(2)	0.29275 (7)	0.22677 (6)	0.25769 (6)	
Ru(3)	0.18490 (7)	0.36780 (6)	0.21730 (6)	
Ru(4)	0.19337 (7)	0.28925 (6)	0.35322 (6)	
P(5)	0.4480 (2)	0.2568 (2)	0.3024 (2)	
P(6)	0.9461 (2)	0.2172 (2)	0.1548 (2)	
C(7)	0.0941 (11)	0.2105 (8)	0.0907 (10)	4.4 (3)
O(8)	0.0864 (9)	0.2121 (7)	0.0215 (9)	7.7 (3)
C(9)	0.1172 (10)	0.1151 (10)	0.2041 (9)	4.5 (3)
O(10)	0.1219 (8)	0.0487 (8)	0.2073 (7)	6.8 (3)
C(11)	0.3102 (10)	0.1385 (8)	0.3089 (9)	3.7 (3)
O(12)	0.3224 (8)	0.0809 (7)	0.3456 (7)	6.6 (3)
C(13)	0.2932 (11)	0.1847 (9)	0.1654 (10)	4.7 (3)
O(14)	0.2926 (9)	0.1538 (8)	0.1070 (9)	7.5 (3)
C(15)	0.2830 (11)	0.4307 (9)	0.2710 (9)	4.4 (3)
O(16)	0.3429 (8)	0.4684 (7)	0.3012 (7)	6.1 (3)
C(17)	0.1578 (11)	0.4014 (9)	0.1117 (10)	4.6 (3)
O(18)	0.1311 (9)	0.4247 (7)	0.0454 (8)	7.3 (3)
C(19)	0.1051 (10)	0.4323 (8)	0.2395 (9)	3.9 (3)
O(20)	0.0568 (7)	0.4750 (6)	0.2524 (6)	5.1 (2)
C(21)	0.2591 (11)	0.3686 (9)	0.4152 (10)	4.5 (3)
O(22)	0.2950 (8)	0.4202 (6)	0.4526 (7)	5.6 (2)
C(23)	0.0868 (10)	0.3271 (8)	0.2581 (9)	3.7 (3)
O(24)	0.0194 (8)	0.3487 (7)	0.3607 (7)	6.1 (3)
C(25)	0.2181 (11)	0.2217 (9)	0.4367 (11)	5.0 (4)
O(26)	0.2411 (8)	0.3186 (7)	−0.0066 (8)	6.4 (3)
C(31)	0.5235 (9)	0.1757 (6)	0.3400 (5)	3.2 (3)
C(32)	0.5965 (9)	0.1775 (5)	0.4138 (5)	4.6 (4)
C(33)	0.6514 (6)	0.1146 (8)	0.4407 (6)	6.1 (4)
C(34)	0.6333 (10)	0.0499 (7)	0.3938 (7)	6.4 (5)
C(35)	0.5604 (10)	0.0481 (5)	0.3200 (7)	6.9 (5)
C(36)	0.5055 (7)	0.1110 (7)	0.2931 (5)	5.1 (4)
C(41)	0.4930 (12)	0.3225 (8)	0.3853 (7)	3.9 (3)
C(42)	0.4764 (11)	0.3084 (7)	0.4551 (8)	5.3 (4)
C(43)	0.5129 (9)	0.3552 (7)	0.5217 (6)	6.7 (5)
C(44)	0.5660 (13)	0.4162 (9)	0.5186 (7)	7.6 (5)
C(45)	0.5826 (11)	0.4304 (7)	0.4489 (9)	7.8 (5)
C(46)	0.5460 (8)	0.3835 (6)	0.3822 (6)	5.3 (4)
C(51)	0.4894 (7)	0.2933 (6)	0.2260 (6)	3.4 (3)
C(52)	0.5789 (7)	0.2814 (6)	0.2341 (6)	6.0 (4)
C(53)	0.6104 (6)	0.3111 (8)	0.1775 (8)	7.5 (5)
C(54)	0.5524 (9)	0.3526 (7)	0.1128 (7)	6.7 (5)
C(55)	0.4628 (8)	0.3645 (6)	0.1047 (6)	4.9 (4)
C(56)	0.4313 (6)	0.3348 (6)	0.1613 (7)	4.7 (4)
C(61)	−0.1104 (10)	0.1647 (6)	0.0612 (6)	4.0 (3)
C(62)	−0.1613 (10)	0.1995 (5)	−0.0114 (8)	5.9 (4)
C(63)	−0.1986 (8)	0.1572 (8)	−0.0815 (6)	7.9 (5)
C(64)	−0.1849 (11)	0.0801 (8)	−0.0791 (7)	8.5 (6)
C(65)	−0.1339 (11)	0.0453 (5)	−0.0065 (9)	6.8 (5)
C(66)	−0.0697 (8)	0.0876 (6)	0.0637 (6)	6.0 (4)
C(71)	−0.1015 (15)	0.3120 (6)	0.1343 (9)	3.2 (3)
C(72)	−0.1514 (10)	0.3424 (5)	0.1762 (7)	4.0 (3)
C(73)	−0.1797 (10)	0.4168 (7)	0.1636 (7)	5.1 (4)
C(74)	−0.1580 (16)	0.4606 (6)	0.1091 (10)	4.7 (4)
C(75)	−0.1081 (11)	0.4302 (5)	0.0671 (7)	5.7 (4)
C(76)	−0.0798 (9)	0.3559 (7)	0.0797 (7)	4.3 (4)
C(81)	−0.1054 (7)	0.1767 (7)	0.2209 (5)	3.1 (3)
C(82)	−0.0517 (5)	0.1618 (7)	0.3012 (6)	4.5 (4)
C(83)	−0.0911 (8)	0.1335 (6)	0.3529 (5)	5.6 (4)
C(84)	−0.1841 (8)	0.1200 (8)	0.3243 (6)	5.9 (4)
C(85)	−0.2377 (6)	0.1349 (8)	0.2441 (7)	5.8 (4)
C(86)	−0.1984 (6)	0.1633 (5)	0.1924 (5)	3.9 (3)

(B) Anisotropic Temperature Factors[a]

Atom	$10^5\beta_{11}$	$10^5\beta_{22}$	$10^5\beta_{33}$	$10^5\beta_{12}$	$10^5\beta_{13}$	$10^5\beta_{23}$
Ru(1)	298 (6)	282 (4)	226 (5)	−21 (4)	124 (4)	3 (3)
Ru(2)	285 (6)	276 (4)	271 (5)	−1 (4)	134 (4)	−2 (3)
Ru(3)	356 (6)	267 (4)	302 (5)	3 (4)	164 (4)	26 (3)
Ru(4)	351 (6)	345 (5)	220 (5)	−17 (4)	132 (4)	−14 (3)
P(5)	210 (18)	273 (15)	289 (16)	−10 (13)	119 (14)	−29 (12)
P(6)	265 (20)	305 (15)	214 (16)	−23 (13)	105 (14)	4 (12)

[a] The form of the Debye-Waller factor is $\exp[-(\beta_{11}h^2 + \beta_{22}k^2 + \beta_{33}l^2 + 2\beta_{12}hk + 2\beta_{13}hl + 2\beta_{23}kl)]$.

Table VI. Bond Distances (Å) in $H_4Ru_4(CO)_{10}(PPh_3)_2$

(a) Ru–Ru (Long) Distances

Ru(1)–Ru(3)	2.9560 (16)	Ru(2)–Ru(3)	2.9827 (16)
Ru(1)–Ru(4)	2.9732 (15)	Ru(2)–Ru(4)	2.9527 (17)
		Av	2.9661 (16)[a]

(b) Ru–Ru (Short) Distances

Ru(1)–Ru(2)	2.7739 (17)	Ru(3)–Ru(4)	2.7698 (16)
		Av	2.7718 (16)[a]

(c) Ru–P Distances

Ru(1)–P(6)	2.362 (4)	Ru(2)–P(5)	2.356 (4)
		Av	2.359 (4)[a]

(d) Ru–C (Pseudo-Trans to the Long M–M Bonds) Distances

Ru(1)–C(7)	1.78 (2)	Ru(3)–C(15)	1.87 (2)
Ru(1)–C(9)	1.82 (2)	Ru(3)–C(19)	1.87 (2)
Ru(2)–C(11)	1.79 (1)	Ru(4)–C(21)	1.86 (2)
Ru(2)–C(13)	1.82 (2)	Ru(4)–C(23)	1.86 (2)
		Av	1.83 (1)[a]

(e) Ru–C (Pseudo-Trans to the Short M–M Bonds) Distances

Ru(3)–C(17)	1.87 (2)	Ru(4)–C(25)	1.84 (2)
		Av	1.85 (2)[a]

(f) Carbonyl Distances

C(7)–O(8)	1.20 (2)	C(9)–O(10)	1.19 (2)
C(11)–O(12)	1.20 (2)	C(13)–O(14)	1.18 (2)
C(15)–O(16)	1.13 (2)	C(17)–O(18)	1.18 (2)
C(19)–O(20)	1.17 (2)	C(21)–O(22)	1.16 (2)
C(23)–O(24)	1.16 (2)	C(25)–O(26)	1.19 (2)
		Av	1.18 (1)[a]

(g) Phosphorus–Carbon Distances

P(5)–C(31)	1.842 (12)	P(5)–C(41)	1.817 (13)
P(5)–C(51)	1.846 (11)	P(6)–C(61)	1.834 (11)
P(6)–C(71)	1.837 (13)	P(6)–C(81)	1.823 (11)
		Av	1.833 (4)[a]

[a] See footnote 29.

evidence for the assignment of triply bridging hydrogens on two opposite faces of the Ru_6 octahedron came from bond-length arguments (two of the triangular faces were larger than the other six), the disposition of carbonyl groups could also have been used to arrive at the same conclusion. A close examination of the CO groups in that compound (reproduced schematically in VIII) shows that, while twelve of the CO

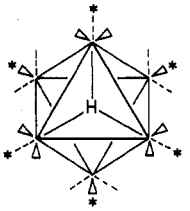

VIII

groups are trans to M–M bonds, the other six (the ones labeled with asterisks) are not. These six, in fact, are placed such that they point at the inferred positions of the triply bridging hydrogen atoms.

For $H_4Ru_4(CO)_{12}$, the three orbitals of VII (which contain a total of two electrons between them) are used to form one Ru–Ru bond and two Ru–H–Ru bridge bonds. It is readily seen that the number of electrons and orbitals in the cluster are just sufficient to form a total of two Ru–Ru bonds and four Ru–H–Ru three-center bonds:

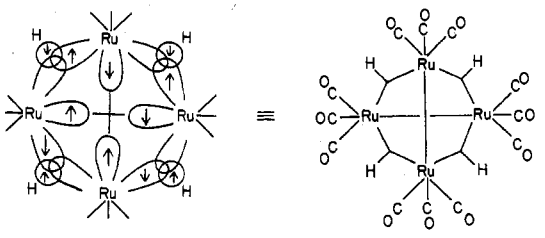

IX

Table VII. Bond Angles (deg) in $H_4Ru_4(CO)_{10}(PPh_3)_2$

	(a) Ru-(short)-Ru-(long)-Ru Angles		
Ru(2)-Ru(1)-Ru(3)	62.64 (4)	Ru(1)-Ru(3)-Ru(4)	62.47 (4)
Ru(2)-Ru(1)-Ru(4)	61.71 (4)	Ru(2)-Ru(3)-Ru(4)	61.63 (4)
Ru(1)-Ru(2)-Ru(3)	61.67 (4)	Ru(1)-Ru(4)-Ru(3)	61.84 (4)
Ru(1)-Ru(2)-Ru(4)	62.46 (4)	Ru(2)-Ru(4)-Ru(3)	62.73 (4)
		Av	62.14 (17)[a]
	(b) Ru-(long)-Ru-(long)-Ru Angles		
Ru(3)-Ru(1)-Ru(4)	55.70 (4)	Ru(1)-Ru(3)-Ru(2)	55.69 (4)
Ru(3)-Ru(2)-Ru(4)	55.63 (4)	Ru(1)-Ru(4)-Ru(2)	55.82 (4)
		Av	55.71 (4)[a]
	(c) Ru-(short)-Ru-P (Pseudo-Trans) Angles		
Ru(2)-Ru(1)-P(6)	171.88 (10)	Ru(1)-Ru(2)-P(5)	170.03 (11)
		Av	170.95 (10)[a]
	(d) Ru-(long)-Ru-P (Pseudo-Cis) Angles		
Ru(3)-Ru(1)-P(6)	112.97 (10)	Ru(3)-Ru(2)-P(5)	108.94 (10)
Ru(4)-Ru(1)-P(6)	110.19 (10)	Ru(4)-Ru(2)-P(5)	116.07 (10)
		Av	112.04 (10)[a]
	(e) Ru-(short)-Ru-C (Pseudo-Trans) Angles		
Ru(4)-Ru(3)-C(17)	165.1 (5)	Ru(3)-Ru(4)-C(25)	165.6 (6)
		Av	165.3 (5)[a]
	(f) Ru-(long)-Ru-C (Pseudo-Trans) Angles		
Ru(3)-Ru(1)-C(9)	152.8 (5)	Ru(1)-Ru(3)-C(15)	148.8 (5)
Ru(4)-Ru(1)-C(7)	147.6 (5)	Ru(2)-Ru(3)-C(19)	147.9 (5)
Ru(3)-Ru(2)-C(11)	146.3 (5)	Ru(1)-Ru(4)-C(21)	149.8 (5)
Ru(4)-Ru(2)-C(13)	150.4 (6)	Ru(2)-Ru(4)-C(23)	149.6 (4)
		Av	149.1 (7)[a]
	(g) Ru-(short)-Ru-C (Pseudo-Cis) Angles		
Ru(2)-Ru(1)-C(7)	96.0 (6)	Ru(4)-Ru(3)-C(15)	95.6 (5)
Ru(2)-Ru(1)-C(9)	88.3 (5)	Ru(4)-Ru(3)-C(19)	86.5 (5)
Ru(1)-Ru(2)-C(11)	95.0 (5)	Ru(3)-Ru(4)-C(21)	88.2 (5)
Ru(1)-Ru(2)-C(13)	88.1 (6)	Ru(3)-Ru(4)-C(23)	96.5 (4)
		Av	91.8 (17)[a]
	(h) Ru-(long)-Ru-C (Pseudo-Cis) Angles		
Ru(3)-Ru(1)-C(7)	94.1 (5)	Ru(3)-Ru(2)-C(13)	109.1 (5)
Ru(4)-Ru(1)-C(9)	110.1 (5)	Ru(4)-Ru(2)-C(11)	92.9 (5)
Ru(1)-Ru(3)-C(17)	103.0 (5)	Ru(1)-Ru(4)-C(23)	95.5 (4)
Ru(1)-Ru(3)-C(19)	107.9 (5)	Ru(1)-Ru(4)-C(25)	111.8 (5)
Ru(2)-Ru(3)-C(15)	95.2 (5)	Ru(2)-Ru(4)-C(21)	109.3 (6)
Ru(2)-Ru(3)-C(17)	114.1 (5)	Ru(2)-Ru(4)-C(25)	102.9 (6)
		Av	103.8 (22)[a]
	(i) P-Ru-C Angles		
P(6)-Ru(1)-C(7)	91.1 (6)	P(5)-Ru(2)-C(11)	94.9 (5)
P(6)-Ru(1)-C(9)	95.6 (6)	P(5)-Ru(2)-C(13)	92.3 (6)
		Av	94.5 (6)[a]
	(j) C-Ru-C Angles		
C(7)-Ru(1)-C(9)	90.9 (7)	C(11)-Ru(2)-C(13)	92.8 (7)
C(15)-Ru(3)-C(17)	99.0 (7)	C(21)-Ru(4)-C(23)	90.7 (7)
C(15)-Ru(3)-C(19)	91.3 (7)	C(21)-Ru(4)-C(25)	96.6 (7)
C(17)-Ru(3)-C(19)	95.7 (7)	C(23)-Ru(4)-C(25)	96.9 (8)
		Av	94.2 (11)[a]
	(k) Ru-P-C Angles		
Ru(2)-P(5)-C(31)	113.7 (4)	Ru(1)-P(6)-C(61)	111.5 (5)
Ru(2)-P(5)-C(41)	117.7 (6)	Ru(1)-P(6)-C(71)	112.4 (7)
Ru(2)-P(5)-C(51)	116.7 (4)	Ru(1)-P(6)-C(81)	120.0 (4)
		Av	115.3 (13)[a]
	(l) C-P-C Angles		
C(31)-P(5)-C(41)	102.0 (6)	C(61)-P(6)-C(71)	105.4 (6)
C(31)-P(5)-C(51)	100.5 (6)	C(61)-P(6)-C(81)	101.8 (6)
C(41)-P(5)-C(51)	103.7 (6)	C(71)-P(6)-C(81)	104.1 (8)
		Av	102.9 (7)[a]
	(m) Ru-C-O Angles		
Ru(1)-C(7)-O(8)	169 (2)	Ru(2)-C(11)-O(12)	178 (1)
Ru(1)-C(9)-O(10)	177 (1)	Ru(2)-C(13)-O(14)	176 (1)
Ru(3)-C(15)-O(16)	178 (1)	Ru(4)-C(21)-O(22)	176 (1)
Ru(3)-C(17)-O(18)	172 (2)	Ru(4)-C(23)-O(24)	178 (1)
Ru(3)-C(19)-O(20)	177 (1)	Ru(4)-C(25)-O(26)	174 (2)
		Av	175.5 (9)[a]

[a] See footnote 29.

Table VIII. Dimensions of the Ru_4 Cores of $H_4Ru(CO)_{12-n}L_n$ Complexes and Related Compounds

$H_4Ru_4(CO)_{12}$[a]	$H_4Ru_4(CO)_{12}$[b]	$H_4Ru_4(CO)_{11}$-$P(OMe)_3$	$H_4Ru_4(CO)_{10}$-$(PPh_3)_2$	$H_4Ru_4(CO)_{10}$-(diphos)[c]	$H_2Ru_4(CO)_{13}$[d]	$H_2Ru_6(CO)_{18}$[e]
			(A) Distances Corresponding to Ru-H-Ru Bonds			
2.945 (1)	2.91 (2)	2.94 (1)	2.953 (2)	2.931 (1)	2.915 (7)	2.950 (3)
2.948 (1)	2.92 (2)	2.94 (1)	2.956 (2)	2.946 (1)	2.947 (6)	2.954 (3)
2.950 (1)	2.93 (2)	2.92 (1)	2.973 (2)	2.988 (1)	2.924 (7)	2.957 (3)
2.956 (1)	2.96 (2)	2.92 (1)	2.983 (2)	3.006 (1)	2.935 (8)	2.952 (3)
Av 2.950	Av 2.93	Av 2.93	Av 2.966	Av 2.968	Av 2.930	2.959 (3)
						2.954 (3)
						Av 2.954
			(B) Distances Corresponding to Ru-Ru Bonds			
2.784 (1)	2.78 (2)	2.76 (1)	2.770 (2)	2.785 (1)	2.785 (7)	2.872 (3)
2.788 (1)	2.82 (2)	2.76 (1)	2.774 (2)	2.796 (1)	2.764 (7)	2.867 (3)
Av 2.786	Av 2.80	Av 2.76	Av 2.772	Av 2.791	2.762 (6)	2.858 (3)
					2.818 (7)	2.874 (3)
					2.771 (7)	2.857 (3)
					2.786 (7)	2.865 (3)
					2.778 (7)	Av 2.867
					2.805 (8)	
					Av 2.784	

[a] 97% occupancy molecule (see text). [b] 3% occupancy molecule (see text). [c] Results for $H_4Ru_4(CO)_{10}(Ph_2PCH_2CH_2PPh_2)$ are taken from ref 18. This molecule differs from all other H_4Ru_4-type compounds in this table in that its two short bonds are adjacent to each other, whereas those in the other molecules are opposite each other. [d] Data taken from ref 21. This molecule has two long bonds (Ru-H-Ru) and four short bonds (Ru-Ru). [e] Data taken from ref 32. In this case, the long distances correspond to Ru-Ru bonds bridged by *triply bridging* hydride ligands.

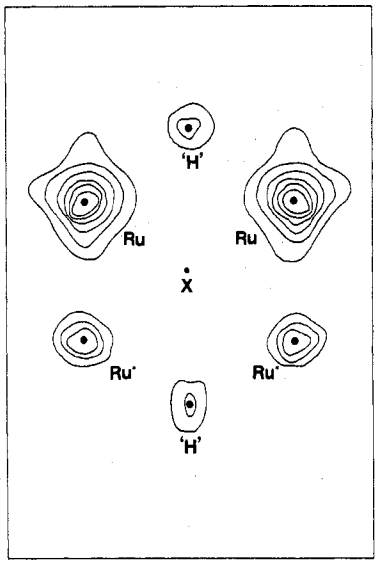

Figure 6. Composite difference Fourier map of the $H_4Ru_4(CO)_{12}$ molecule. This map is a composite synthesized in a similar manner to that of ref 4 except that only four planes are averaged. They are those containing a molecular twofold axis (but no mirror plane) and two 97% occupancy Ru atoms separated by a "long bond". X denotes the tetramer center. The symbol Ru represents the 97% occupancy ruthenium position and Ru* corresponds to the 3% occupancy position. The "H" peaks might conceivably be assigned to edge-bridging hydride atoms between the Ru atoms illustrated at the top of the diagram and between the two perpendicular Ru atoms (not shown) which are above and below the plane of the diagram near the bottom. But these positions cannot be considered conclusive (see text) even though they yield reasonable measured metal–hydrogen distances of 1.76 Å. Contours start at 0.3 e $Å^{-3}$ with 0.2 e $Å^{-3}$ increments for this map which was calculated with all data.

The bonding in $H_4Ru_4(CO)_{12}$ can thus be symbolized by IX, where the Y-shaped connecting lines are used to represent three-center two-electron M–H–M bonds.[39] In contrast, $H_4Re_4(CO)_{12}$ has four fewer electrons. Instead of having the 16 orbitals and 12 electrons used by $H_4Ru_4(CO)_{12}$ to form two M–M bonds and four M–H–M bonds (as shown in IX), $H_4Re_4(CO)_{12}$ has 16 orbitals and only 8 electrons. One alternative is to form four M_3H four-center/two-electron bonds, which is a way of rationalizing the face-bridging structure of $H_4Re_4(CO)_{12}$.

As mentioned earlier, one interesting feature of the chemistry of $H_4Ru_4(CO)_{12}$ is the feasibility with which the hydrogen atoms move around the cluster.[13,18] This implies, of course, that the energy barrier for such tautomerization must be very low. One can imagine a number of pathways involving hydrogen transfer into the vacant edge-bridging or face-bridging positions or even direct tunnelling through the M_4 cluster itself. The edge ↔ face mechanism finds some support from the known structure of $H_4Co_4(C_5H_5)_4$, a 60-electron saturated cluster with face-bridging hydrogen atoms.[40] However, Shapley has presented NMR evidence which implicates a terminally bonded hydride intermediate in the rearrangement.[18]

Hoffmann and co-workers have recently analyzed the energetics of face-bridging vs. edge-bridging structures for staggered (V) and eclipsed (VI) $H_4M_4(CO)_{12}$ clusters.[41] They conclude that for the staggered configuration there is not much difference energetically between edge protonation and face protonation. However, for the eclipsed conformation there is a pronounced preference for face-bridging hydrogen atoms.

Acknowledgment. This research was supported by NSF Grants CHE-74-01541 and CHE-77-00360. Computer time was supplied by the USC Computing Center. R. B. acknowledges support from an Alfred P. Sloan Fellowship (1974–1976) and an NIH Research Career Development Award (1975–1980) during the course of this work.

Registry No. $H_4Ru_4(CO)_{12}$, 34438-91-0; $H_4Ru_4(CO)_{10}(PPh_3)_2$, 65899-42-5; $Ru_3(CO)_{12}$, 15243-33-1.

Supplementary Material Available: Listings of the observed and calculated structure factor amplitudes for both structures (34 pages). Ordering information is given on any current masthead page.

References and Notes

(1) *Adv. Chem. Ser.*, **No. 167** (1978).
(2) (a) H. D. Kaesz, *Chem. Br.*, **9**, 344 (1973); (b) H. D. Kaesz and R. B. Saillant, *Chem. Rev.*, **72**, 231 (1972).
(3) For example: (a) Terminal M–H bond: $H_2Os_3(CO)_{11}$ [M. R. Churchill and B. G. De Boer, *Inorg. Chem.*, **16**, 878 (1977)]. (b) Bridging M–H–M bond: $H_3Mn_3(CO)_{12}$ [S. W. Kirtley, J. P. Olsen, and R. Bau, *J. Am. Chem. Soc.*, **95**, 4532 (1973)]. (c) Triply bridging HM_3 bond: $HFeCo_3(CO)_9(P(OCH_3)_3)_3$ [B. T. Huie, C. B. Knobler, and H. D. Kaesz, *J. Chem. Soc., Chem. Commun.*, 684 (1975)]. (d) "Interstitial" H atom: HNb_6I_{11} [A. Simon, *Z. Anorg. Allg. Chem.*, **355**, 311 (1976)];

$[HNi_{12}(CO)_{21}]^{3-}$ and $[H_2Ni_{12}(CO)_{21}]^{2-}$ [R. W. Broach, L. F. Dahl, G. Longoni, P. Chini, A. J. Schultz, and J. M. Williams, *Adv. Chem. Ser.*, **No. 167** (1978)].
(4) R. D. Wilson and R. Bau, *J. Am. Chem. Soc.*, **98**, 2434 (1976).
(5) B. F. G. Johnson, R. D. Johnston, J. Lewis, and B. H. Robinson, *Chem. Commun.*, 851 (1966).
(6) J. W. S. Jamieson, J. V. Kingston, and G. Wilkinson, *Chem. Commun.*, 569 (1966).
(7) B. F. G. Johnson, R. D. Johnston, J. Lewis, B. H. Robinson, and G. Wilkinson, *J. Chem. Soc. A*, 2856 (1968).
(8) The T_d structure contained face-bridging hydride ligands, the D_{2d} structure contained edge-bridging hydride ligands, and the three C_{3v} structures each contained one "body-centered" hydride ligand plus edge-bridging or face-bridging hydrides.[3]
(9) B. F. G. Johnson, J. Lewis, and P. A. Kilty, *J. Chem. Soc. A*, 2859 (1968).
(10) J. R. Moss and W. A. G. Graham, *J. Organomet. Chem.*, **23**, C47 (1970).
(11) H. D. Kaesz, S. A. R. Knox, J. W. Koepke, and R. B. Saillant, *Chem. Commun.*, 477 (1971).
(12) S. A. R. Knox, J. W. Koepke, M. A. Andrews, and H. D. Kaesz, *J. Am. Chem. Soc.*, **97**, 3942 (1975).
(13) S. A. R. Knox and H. D. Kaesz, *J. Am. Chem. Soc.*, **93**, 4594 (1971).
(14) F. Piacenti, M. Bianchi, P. Frediani, and E. Benedetti, *Inorg. Chem.*, **10**, 2759 (1971).
(15) J. W. Koepke, J. R. Johnson, S. A. R. Knox, and H. D. Kaesz, *J. Am. Chem. Soc.*, **97**, 3947 (1975).
(16) (a) E. L. Muetterties, *Science*, **196**, 839 (1977); (b) A. L. Robinson, *ibid.*, **194**, 1150, 1261 (1976).
(17) R. M. Laine, R. G. Rinker, and P. C. Ford, *J. Am. Chem. Soc.*, **99**, 252 (1977).
(18) J. R. Shapley, S. I. Richter, M. R. Churchill, and R. A. Lashewycz, *J. Am. Chem. Soc.*, **99**, 7384 (1977).
(19) R. Saillant, G. Barcelo, and H. D. Kaesz, *J. Am. Chem. Soc.*, **92**, 5739 (1970).
(20) B. F. G. Johnson, J. Lewis, and I. G. Williams, *J. Chem. Soc. A*, 901 (1970).
(21) D. B. W. Yawney and R. J. Doedens, *Inorg. Chem.*, **11**, 838 (1972).
(22) See footnote 24 in ref 4.
(23) H. B. Chin and R. Bau, *J. Am. Chem. Soc.*, **98**, 2434 (1976).
(24) (a) T. C. Furnas, "Single Crystal Orienter Manual", General Electric Co., Milwaukee, Wis., 1966; (b) P. W. R. Corfield, R. J. Doedens, and J. A. Ibers, *Inorg. Chem.*, **6**, 197 (1967).
(25) Phenyl rings were defined as ideal hexagons with C–C distances of 1.394 Å. Rigid-body parameters are calculated according to R. J. Doedens, in "Crystallographic Computing", F. R. Ahmed, Ed., Munksgaard, Copenhagen, 1970, pp 198–200.
(26) (a) Most of the major computations in this work were performed using CRYM, an amalgamated set of crystallographic programs developed by R. E. Marsh and his group at the California Institute of Technology. Rigid-body least-squares refinement was carried out with UCIGLS (adapted by R. J. Doedens and J. A. Ibers from W. R. Busing and H. A. Levy's ORFLS), and molecular plots were calculated with ORTEP (by C. K. Johnson). All calculations were carried out at the USC IBM 370/158 computer. (b) $R = \sum||F_o| - |F_c||/\sum|F_o|$ and $R_w = [\sum w(|F_o| - |F_c|)^2/\sum wF_o^2]^{1/2}$, where the weights w are defined as $4F_o^2/[\sigma(F_o^2)]^2$. All refinements were carried out on F.
(27) The occupancy (p) of one Ru_4 core is allowed to vary between 0 and 1 and the second orientation occupancy is set to $1 - p$. However only 12 full-occupancy carbonyls (corresponding to the major occupancy Ru_4 orientation) were included in the model since refinement at the 3% occupancy level of CO's was assumed to be prohibitively difficult and final difference Fourier maps gave no indication that such a treatment was necessary.
(28) (a) S. J. LaPlaca, and J. A. Ibers, *Acta Crystallogr.*, **18**, 511 (1965); (b) S. W. Kirtley, J. P. Olsen, and R. Bau, *J. Am. Chem. Soc.*, **95**, 4532 (1973).
(29) For the averaged values obtained from six or more measurements the errors are found by $\sigma = [\sum(x_i - \bar{x})^2/n(n-1)]^{1/2}$ (where x_i and $\bar{x}$ are the individual and mean values, respectively). For the other mean values the σ is simply the average of the individual estimated standard deviations (in parentheses) derived from the final least-squares refinement.
(30) Supplementary material.
(31) M. R. Churchill, P. H. Bird, H. D. Kaesz, R. Bau, and B. Fontal, *J. Am. Chem. Soc.*, **90**, 7135 (1968).
(32) M. R. Churchill and J. Wormald, *J. Am. Chem. Soc.*, **93**, 5670 (1971).
(33) R. Bau, B. C. K. Chou, S. A. R. Knox, V. Riera, and F. G. A. Stone, *J. Organomet. Chem.*, **82**, C43 (1974).
(34) M. R. Churchill, F. J. Hollander, and J. P. Hutchinson, *Inorg. Chem.*, **16**, 2655 (1977).
(35) B. A. Coyle and J. A. Ibers, *Inorg. Chem.*, **11**, 1105 (1972).
(36) (a) C. H. Wei, and L. F. Dahl, *J. Am. Chem. Soc.*, **91**, 1351 (1969); (b) C. H. Wei, *Inorg. Chem.*, **8**, 2384 (1969).
(37) H. D. Kaesz, B. Fontal, R. Bau, S. W. Kirtley, and M. R. Churchill, *J. Am. Chem. Soc.*, **91**, 1021 (1969).
(38) M. Elian, M. M. L. Chen, D. M. P. Mingos, and R. Hoffmann, *Inorg. Chem.*, **15**, 1148 (1976).
(39) J. P. Olsen, T. F. Koetzle, S. W. Kirtley, M. Andrews, D. L. Tipton, and R. Bau, *J. Am. Chem. Soc.*, **96**, 6621 (1974).
(40) G. Huttner and H. Lorenz, *Chem. Ber.*, **108**, 973 (1975).
(41) R. Hoffmann, B. E. R. Schilling, R. Bau, H. D. Kaesz, and D. M. P. Mingos, *J. Am. Chem. Soc.*, in press.

Contribution from the Department of Chemistry,
The University of Notre Dame, Notre Dame, Indiana 46556

Molecular Stereochemistry of Two Binuclear Metalloporphyrins Containing the $M_2O_3^{4+}$ Unit. μ-Oxo-bis(oxo-$\alpha,\beta,\gamma,\delta$-tetraphenylporphinatomolybdenum(V)) and Tri-μ-oxo-bis($\alpha,\beta,\gamma,\delta$-tetraphenylporphinatoniobium(V))[1]

JAMES F. JOHNSON and W. ROBERT SCHEIDT*

Received September 9, 1977

The molecular stereochemistry of two binuclear metalloporphyrins with molecular formula $[O_3M_2(TPP)_2]$, where M = Nb(V) or Mo(V) and TPP is the dianion of $\alpha,\beta,\gamma,\delta$-tetraphenylporphyrin, have been determined by x-ray diffraction techniques using counter data. Crystal data: $O_3Nb_2(TPP)_2$, monoclinic, space group Cc, $Z = 4$, $a = 10.765$ (5) Å, $b = 24.913$ (6) Å, $c = 29.332$ (8) Å, $\cos\beta = -0.3794$ (4); $O_3Mo_2(TPP)_2$, monoclinic, space group $C2/c$, $Z = 4$, $a = 18.211$ (2) Å, $b = 19.309$ (3) Å, $c = 28.989$ (3) Å, $\cos\beta = -0.4320$ (1). Refinement of the niobium complex was based on 5748 observed data, final discrepancy indices $R_1 = 0.063$ and $R_2 = 0.073$. Refinement of the molybdenum complex was based on 7742 observed data, final discrepancy indices $R_1 = 0.059$ and $R_2 = 0.089$. The niobium complex is seven-coordinate with three bridging oxygen ligands. Unique Nb–O distances are 1.910, 1.990, 1.760, 1.782, 2.278, and 2.440 Å. The average Nb–N bond distance is 2.246 Å. The Nb–Nb separation is 2.872 Å. The molybdenum complex is six-coordinate; the $Mo_2O_3^{4+}$ unit has the unusual geometry of a linear five-atom grouping with two terminal Mo=O groups and a single Mo—O—Mo bridge. The Mo—O distances are 1.707 and 1.936 Å. This unusual arrangement for a binuclear Mo(V) complex leads to a paramagnetic species. The average Mo—N bond distance is 2.094 Å.

The early transition element metalloporphyrin derivatives frequently have as axial ligand(s) strongly bound oxygen atom(s) and form both mononuclear and binuclear complexes. Oxometalloporphyrin derivatives of niobium(V), tungsten(V), rhenium(V), and molybdenum(V) have been report by Buchler and co-workers.[2,3] Molybdenum(V) derivatives were first reported by Fleischer.[4] Niobium(V) derivatives have also been recently reported by Guilard et al.[5] One class of derivatives for all these metal ions has empirical formula $O_3M_2(P)_2$ where P is either the dianion of octaethylporphyrin or tetraphenylporphyrin. We have determined the molecular structure of two such derivatives where M is either niobium(V) or

0020-1669/78/1317-1280$01.00/0